Materiales de Construcción
Vol. 65, Issue 320, October–December 2015, e069
ISSN-L: 0465-2746
http://dx.doi.org/10.3989/mc.2015.05414

Behaviour of FRP confined concrete in square columns

A. de Diego[a]✉, A. Arteaga[a], J. Fernández[b], R. Perera[b], D. Cisneros[a]

a. Eduardo Torroja Institute for Construction Science, CSIC, Madrid, Spain
b. Technical University of Madrid, Madrid, Spain
✉adediego@ietcc.csic.es

Received 6 August 2014
Accepted 16 April 2015
Available on line 23 September 2015

ABSTRACT: A significant amount of research has been conducted on FRP-confined circular columns, but much less is known about rectangular/square columns in which the effectiveness of confinement is much reduced.

This paper presents the results of experimental investigations on low strength square concrete columns confined with FRP. Axial compression tests were performed on ten intermediate size columns. The tests results indicate that FRP composites can significantly improve the bearing capacity and ductility of square section reinforced concrete columns with rounded corners. The strength enhancement ratio is greater the lower the concrete strength and also increases with the stiffness of the jacket.

The confined concrete behaviour was predicted according to the more accepted theoretical models and compared with experimental results. There are two key parameters which critically influence the fitting of the models: the strain efficiency factor and the effect of confinement in non-circular sections.

KEYWORDS: Concrete; Composite; FRP; Confinement; Compressive strength

Citation/Citar como: de Diego, A.; Arteaga, A.; Fernández, J.; Perera, R.; Cisneros, D. (2015) Behaviour of FRP confined concrete in square columns. *Mater. Construcc.* 65 [320], e069 http://dx.doi.org/10.3989/mc.2015.05414.

RESUMEN: *Comportamiento de hormigón confinado con FRP en pilares cuadrados*. La mayoría de las investigaciones sobre hormigón confinado con FRP se han realizado sobre pilares de sección circular, pero el comportamiento en secciones cuadradas/rectangulares, donde el confinamiento es menos eficaz, es mucho menos conocido.

Este trabajo presenta los resultados de un estudio experimental sobre probetas de hormigón de baja resistencia y sección cuadrada. Se han ensayado a compresión centrada diez probetas de tamaño intermedio. Los resultados indican que el confinamiento mejora significativamente la resistencia y ductilidad del hormigón en columnas de sección cuadrada con las esquinas redondeadas. El incremento de resistencia es mayor cuanto menor es la resistencia del hormigón sin confinar y también aumenta con la rigidez del encamisado.

Los resultados se compararon con los obtenidos según los modelos teóricos más aceptados. Hay dos parámetros críticos en el ajuste de los modelos: el factor de eficiencia de la deformación y el efecto de confinamiento en secciones no circulares.

PALABRAS CLAVE: Hormigón; Composite; FRP; Confinamiento; Resistencia a la compresión

1. INTRODUCTION

The strengthening of reinforced concrete structures using fibre reinforced polymers (FRP) has been widely studied over the last few decades (1–4). One of the most attractive applications of FRP is the confinement of concrete columns to enhance both strength and ductility. The first significant FRP strengthening applications in columns were made in the 1980s in seismic areas, as appropriate confinement increases the ductility, but the confinement is also effective in non-seismic areas due to the

increased axial load capacity of the columns. In the last thirty years there has been a significant research effort in this field, as the number of applications worldwide has grown and many design guidelines have been published for strengthening structures with FRP including column confinement (5–8).

In all these applications, the FRP strengthening is placed, according to various techniques, so that the fibres are wrapped around the pillar, mainly perpendicularly to its axis. When a concrete column is axially compressed, by the so-called Poisson effect, the concrete expands laterally and this expansion is restrained by the FRP. The FRP provides a lateral confinement pressure and the concrete column is subjected to a triaxial stress state.

Studies to date, both experimental and analytical, have led to the development of stress-strain models of two types: design-oriented models, where axial compression strength, ultimate axial deformation and final stress-strain behaviour are predicted using closed-form expressions, obtained by fitting experimental results (9–11); and analysis-oriented ones, in which the stress-strain response model is obtained using an iterative numerical procedure (12–16).

Also, some studies have been published comparing the proposed models with larger data-bases of experimental results collected from the literature, or with new own tests (17–19), finding significant differences in the fit of the models. Comparative studies indicate the dispersion found in the analysed test results in cylindrical specimens, which are the most abundant, and, besides, the scarcity of experimental studies including: specimens of square or rectangular cross-section; large-scale, or at least intermediate, elements; and specimens with low concrete strength, of the order of 20 MPa or less, which can be found in the rehabilitation of old structures.

Certainly, experimental studies on non-cylindrical specimens are much scarcer (20–22), and, predictably, show that confinement is less effective. For the theoretical analysis, models developed for cylindrical specimens, adapted by introducing shape factors, are generally used (5–8, 23).

In order to increase knowledge about the behaviour of columns of reinforced concrete with square cross-section externally reinforced with FRP under centred compression, an experimental study has been carried out, the results of which are presented in this article, as well as a comparison with the most accepted models that have been adopted by the existing design guidelines.

2. EXPERIMENTAL PROGRAMME

Axial compression tests were performed on ten intermediate size columns. The specimens were cast with concrete of different compressive strengths, and strengthened by hand lay-up of FRP sheets.

Concrete with lower than 20 MPa strength has been used in this study, because in the literature there is a lack of available results of low strength concrete, and, at the same time, is the most common strength found in rehabilitation of old structures.

2.1. Description of the specimens

Test specimens were formed by a central part with a length of 600 mm and a square section of 150×150 mm^2 and two 400×400×140 mm^3 heads on the ends (Figure 1). The heads simulated the connection with the top and bottom floor slabs or foundations, and served to prevent premature failure at the extremes of specimen. The cross-section of the column had rounded corners with a 25 mm radius of curvature.

The value of the concrete compressive strength was obtained by testing at 28 days after casting cylindrical normalized specimens (150 mm diameter and 300 mm height) for each series (5 series). The longitudinal reinforcement was made up of four 6 mm diameter steel bars, and 6 mm diameter stirrups were spaced at 100 mm. The yield stress of the steel reinforcement was 500 N/mm^2.

Each series consisted of two specimens cast with the same concrete: one specimen was strengthened with two layers of glass fibre and the other one with a layer of carbon fibre. The FRP was applied by the hand lay-up technique which is the most common strengthening method. After removing the dust and dirt from the surface of the specimen, a layer of epoxy resin was placed on the specimen, then the fibre was wrapped around it with a length of 100 mm overlap and finally another layer of resin epoxy was applied. Fibres were placed perpendicularly to the axis of the column, in what is called a 0° orientation. Table 1 shows the fibres mechanical properties according to the manufacturer technical data sheets, and the FRP properties obtained by means of tensile testing of flat coupons according to (24).

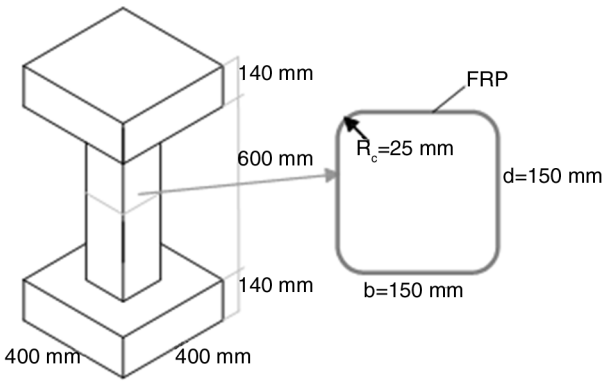

FIGURE 1. Specimen geometry.

TABLE 1. Mechanical properties of strengthening materials

Material	Tensile strength [MPa]	Elastic Modulus [MPa]	Thickness [mm]
Carbon fibre[(1)]	3800	242000	0.3
CFRP[(2)]	818.6	55048	1.2
Glass fibre[(1)]	2600	70000	0.4
GFRP[(2)]	702.6	20493	1.3

[(1)]Properties referred to the fibre itself.
[(2)]Properties referred to the total area of the system.

Thereafter the specimens were named as follows: a letter indicating the type of jacket (C for carbon and G for glass) followed by a number from 1 to 5 indicating the series number, with series 1 with the lowest strength (f_{co}=8.8 MPa) and series 5 the larger one (f_{co}=17.5 MPa).

2.2. Test set-up and instrumentation

The specimens were tested with centred compression load in a 1000 kN capacity INSTRON press. The specimens were placed in the press with a thin layer of plaster applied to both ends (between the lower end and the base of the press and between the upper end and the load application plate) for the purpose of levelling the specimen and eliminating irregularities at the end surfaces.

The load was applied on a 150×150×20 mm^3 steel plate centred on the head of the jack coinciding with the section of the column. The test was carried out in displacement controlled way until failure.

To measure the axial deformation of the column four linear transducers (LVDT) with a 5 mm range and 0.001 mm precision were used. The transducers were placed between the heads of the column, 160 mm away from its axis, centred to each face (Figure 2).

To measure the transverse strain, electrical strain gauges were glued onto the FRP jacket at half the height of the specimen. Four strain gauges were used centred at each face, perpendicularly to the column axis, that is, in the fibre direction.

The measurements of the transducers, strain gauges, and the applied load were continuously recorded during the tests. In series 1 and 3 lateral deformation was not measured, and also in specimen C1 one error occurred and the axial strain was not recorded.

3. RESULTS

3.1. Experimental results

The results are summarized in Table 2. Indicated for each specimen is: the unconfined concrete strength obtained from cylindrical standard samples (f_{co}), the ultimate axial stress (f_{cc}), the relationship between these two magnitudes (f_{cc}/f_{co}), the ultimate axial (ε_{cc}) and lateral (ε_l) strain and the relationship between this last and the ultimate deformation obtained in the tensile coupon test ($\varepsilon_l/\varepsilon_j$).

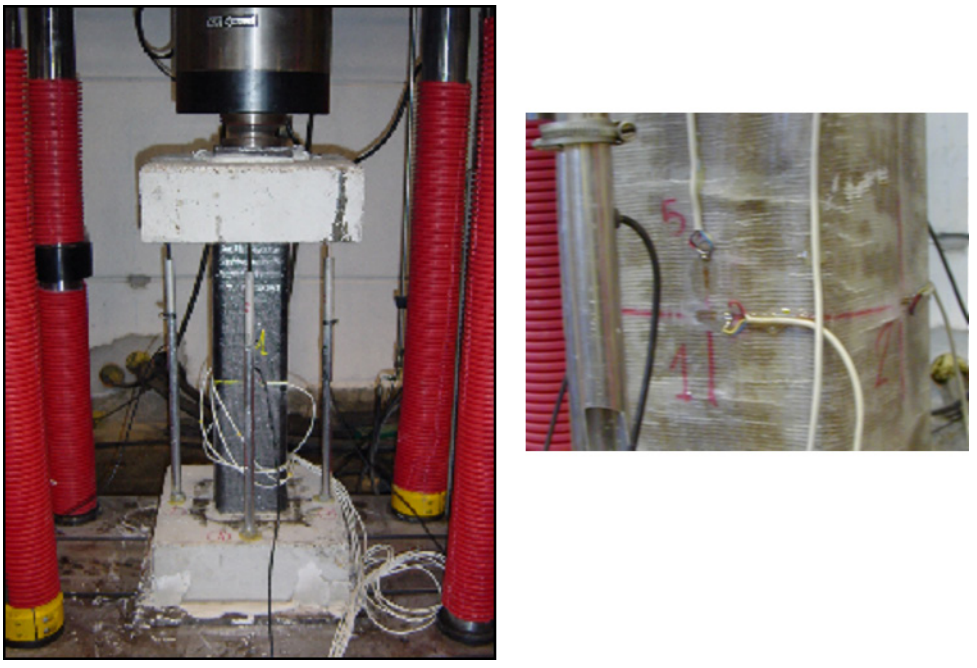

FIGURE 2. Test set-up and instrumentation.

TABLE 2. Test results

Specimen	f_{co} [MPa]	f_{cc} [MPa]	f_{cc}/f_{co}	ε_{cc} [mm/m]	ε_l [mm/m]	$\varepsilon_l/\varepsilon_j$
C1	8.8	22.23	2.53	–	–	–
G1	8.8	19.35	2.20	28.67	–	–
C2	13	23.48	1.81	41.29	−4.90	0.33
G2	13	19.21	1.48	35.12	−4.88	0.14
C3	16.3	28.29	1.71	31.20	–	–
G3	16.3	24.89	1.51	19.67	–	–
C4	16.5	29.11	1.74	24.16	−4.65	0.31
G4	16.5	24.22	1.45	23.68	−10.37	0.30
C5	17.5	25.82	1.48	28.85	−4.39	0.29
G5	17.5	24.56	1.40	28.61	−12.55	0.37

The ultimate concrete axial stress was calculated by subtracting the contribution of the longitudinal reinforcement (area of the four bars multiplied by their yielding stress) from the ultimate load, and dividing the result by the area of the net concrete cross-section. The values of the ultimate axial and transverse strains were obtained as the mean value of the readings of the four transducers or four gauges, respectively, located in the midsection of the specimen. Positive values indicate compressive strain and negative values tension.

Shown for each specimen in Figure 3 are the axial stress vs. average longitudinal and lateral strain curves obtained as average readings of displacement transducers and strain gauges respectively. During the loading of specimen C4, the test had to be stopped, and the specimen was unloaded and reloaded again. Only the second part of the test is shown in the figure.

The failure of the specimens was caused in all cases by the jacket rupture, usually near a corner (Figure 4). The failure occurred suddenly, although previously some warning signals such as noise and "wrinkles" in the jacket were noted. These wrinkles were more visible on glass jackets (where can be appreciated whiter areas indicating debonding of the jacket).

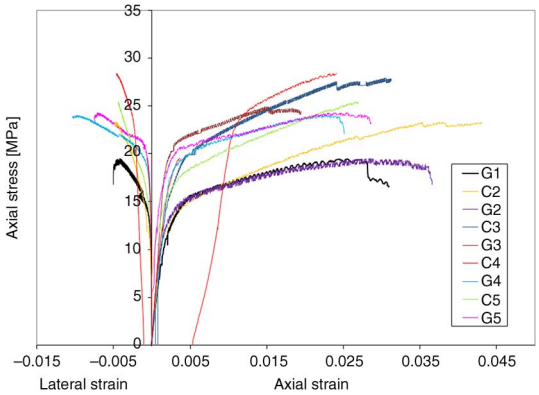

FIGURE 3. Experimental stress-strain curves.

3.2. Analysis of experimental results

The test results (Table 2) show that confinement with FRP significantly improves the axial load capacity and ductility in all specimens.

The lower the unconfined concrete strength (f_{co}), the greater the strength enhancement ratio (f_{cc}/f_{co}). It also increases with the stiffness of the jacket (it is higher for carbon fibre strengthening than for glass fibre). The value of the ratio f_{cc}/f_{co} obtained in the test varies between 1.40 for the concrete strength of 17 MPa confined with glass fibres and 2.53 for the 8.8 MPa concrete strength confined with carbon.

In Figure 3 it can be seen that the axial and lateral stress-strain curves obtained in all the tests have a very similar pattern, approximately a bilinear form, as predicted by the models, with a smooth transition zone. In the first part of the curve, behaviour is very similar to what unconfined concrete would have. In this part, with axial stress below the unconfined concrete strength, the lateral expansion of the concrete core is small and not enough to put the fibre strengthening in tension. In the second part of the curves, with the concrete already cracked, the confinement due to the FRP jacket significantly influences the behaviour of the specimens. In all cases, the second branch is also upward, reaching the maximum load and deflection at the time of failure. It is observed that the slope of the second branch is approximately equal in all specimens confined with glass, and equally in those with carbon.

The strains measured on the fibres at the time of rupture are significantly lower than the ultimate strains obtained by standard tensile testing of FRP flat coupons. This fact is shown in most of the published experimental studies (11, 25–26) and may be related to the triaxial stress state on jackets, the curvature of the fibres and also to local stress concentrations in the fibres caused by the cracked concrete. Several design guidelines and authors have proposed introducing a coefficient of efficiency applied to the ultimate strain to account for this fact, although there is no unanimity in the proposed value.

The value of the ultimate lateral strains shown in Table 2 is the average value measured at the four faces, which corresponds to the last point of the stress-strain curves of Figure 3. The relationship between this value and the ultimate strain obtained in tensile tests on coupons ranges approximately between 14 and 37%, with a mean value of 29%. However, it is difficult to propose a coefficient of efficiency of the ultimate strain that would apply generally, due to the fact that if we observe the measured strains for each gauge just before the failure, some gauges reach values well above these mean values, and besides, the number of tests is small.

As mentioned before, all the specimens failed in a similar manner due to the rupture of the jackets.

FIGURE 4. Failure of specimens.

There has been no failure due to debonding in the jacket overlap. The overlap length of 100 mm is sufficient for the size of the specimens.

4. COMPARISON OF THE EXPERIMENTAL RESULTS WITH MODELS OR GUIDELINES

In this section the tests results are compared with the theoretical values calculated according to two models: an analytical model, proposed by Spoelstra and Monti (12) (included in *fib* Bulletin 14 (5)), and an empirical model, proposed by Lam and Teng (11) (included in some other proposals and design guidelines (7–8)).

4.1. Spoelstra and Monti's model

In *fib* Bulletin 14 Spoelstra & Monti's model is proposed as the most versatile despite its operational complexity. It is an analytical model which combines the Mander's model (27), for concrete confined with steel, with a model expressing the lateral strain as a

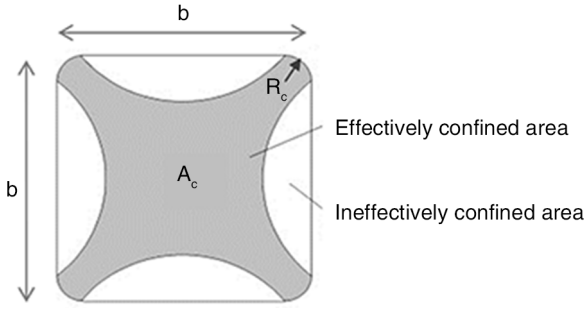

FIGURE 5. Confinement on square cross-sections.

function of the axial strain, to take into account the specific behaviour of FRP. The complete stress-strain curve may be considered as formed by the points of a curve crossing a family of Mander's curves, each one belonging to the pressure level corresponding to the lateral confinement strain at each moment, while the ultimate stress and strain can be obtained from the confining pressure exerted by the jacket at the ultimate load.

The model considers that the ultimate axial strain occurs when the lateral strain of the concrete reaches the value of the ultimate strain of the FRP (subjected to a multiaxial state of stress) and the jacket fails. It gives no indication as to how to obtain the value of the ultimate strain. In this comparison we have calculated this strain using a strain efficiency factor k_ε=0.6, i.e., expressed as the ratio of the jacket ultimate hoop strain to the failure strain determined according to flat coupon tensile tests. This value of k_ε was chosen because it is approximately equal to that obtained by several authors from analysis of tests from the literature (11, 28).

Regarding the influence of the shape of the cross-section, we have calculated this by introducing two different form factors into the model:

- The form factor based on the arc-effect, the most commonly accepted, proposed in *fib* Bulletin 14, which considers as confined only the area of concrete contained by four quadratic parabolas intersecting the sides at 45°, while at the rest of the cross-section the confinement is negligible (Figure 5). In this case, as the ratio of the enclosed area and the total area of concrete, a factor α_e=0.695 is obtained.
- A form factor proposed by Mirmiran (29) and others (30) that for square sections would be given by $\alpha_e=2R_c/b$, yielding values of α_e much smaller, and more influenced by the radius of curvature on the corners. In the case of tested specimens α_e=0.333.

Table 3 shows the experimental and theoretical values of f_{cc}/f_{co} and ε_{cc} for both values of α_e. When considering α_e=0.695, the strength in all specimens is overestimated, with an average error of 40.8% in f_{cc}/f_{co} and 86.9% in ε_{cc}. The best estimates of strength and strain are achieved with α_e=0.333, where the absolute error is 8.3% in the strength and 52.6% in the axial strain.

Figure 6 shows the axial stress versus axial and transverse strain curves obtained experimentally in two specimens of the series 2 compared with those obtained by the iterative procedure given by Spoelstra & Monti with the two values of α_e: α_e=0.695 and α_e=0.333. It is observed that the model reproduces well the shape of the experimental curves, and the slope of the second branch, while overestimating the ultimate strength and strain when adopting α_e=0.695,

TABLE 3. Comparison between the experimental and the theoretical results according to Spoelstra and Monti's model

	f_{cc}/f_{co}			ε_{cc}		
		k_ε=0.6			k_ε=0.6	
Specimen	**Exper.**	**α_e=0.695**	**α_e=0.333**	**Exper.**	**α_e=0.695**	**α_e=0.333**
C1	2.53	2.96	2.24	–	0.0406	0.0308
G1	2.20	2.77	2.08	0.0287	0.0858	0.0644
C2	1.81	2.56	1.93	0.0413	0.0329	0.0247
G2	1.48	2.37	1.76	0.0351	0.0682	0.0506
C3	1.71	2.34	1.76	0.0312	0.0285	0.0215
G3	1.51	2.14	1.59	0.0152	0.0583	0.0432
C4	1.74	2.32	1.75	0.0242	0.0283	0.0213
G4	1.45	2.13	1.58	0.0237	0.0578	0.0428
C5	1.48	2.28	1.72	0.0289	0.0275	0.0207
G5	1.40	2.09	1.55	0.0286	0.0560	0.0415
Error(%)		40.8	8.6		86.9	52.6

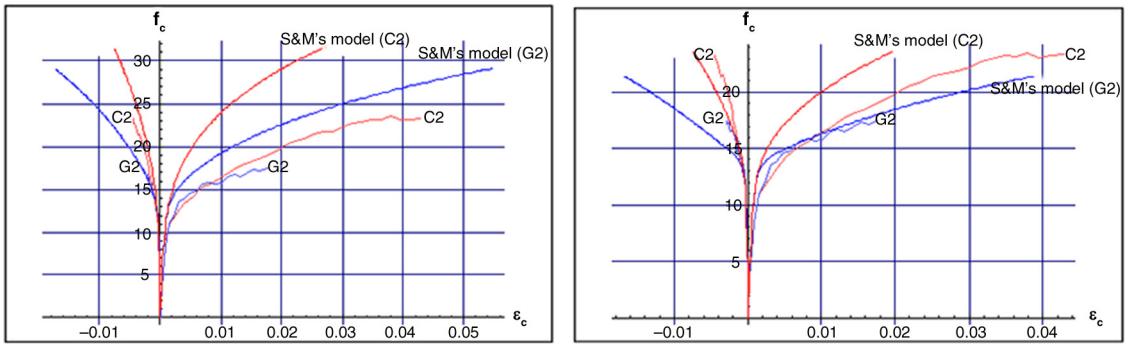

FIGURE 6. Comparison between Spoelstra and Monti's model with two shape factors and experimental results for specimens C2 and G2.

and fits much better adopting α_e=0.333. The graphs for other specimens show a very similar pattern and are not included.

4.2. Lam and Teng's model

Lam and Teng (23) proposed a model for rectangular sections derived from the model by the same authors for circular sections (11), based on an extensive database obtained from experimental results in the literature. In the model the stress-strain curve is formed by a first parabolic and a second linear branch.

The ultimate strength and strain of concrete for rectangular cross-sections is calculated by the following equations [1] [2]:

$$f_{cc} = f_{co} + 3.3 k_{s1} f_l \quad [1]$$

$$\frac{\varepsilon_{cc}}{\varepsilon_{co}} = 1.75 + 12 k_{s2} \frac{f_l}{f_{co}} \left(\frac{\varepsilon_{ju}}{\varepsilon_{co}} \right)^{0.45} \quad [2]$$

In these equations f_l is the maximum confining pressure given by the FRP jacket to an equivalent circular column with a diameter equal to the length of the diagonal of the rectangular section. In calculating the values of the ultimate FRP effective strain to be used in the jacket, from the analysis of experimental results from the literature, Lam and Teng proposed a value of k_ε=0.586 for carbon and k_ε=0.624 for glass fibres, while indicating the large observed dispersion.

k_{s1} and k_{s2} are the two shape factors that depend on the relationship between the dimensions of the sides of the section and the effectively confined area ratio, whereas this model considers the area bounded by the parabolas intersecting the sides of the rectangle parallel to the slope of the diagonal section. For the particular case of square sections, k_{s1} and k_{s2} have the same value and also match the factor α_e proposed in *fib* Bulletin 14. In the specimens tested k_{s1}=k_{s2}=0.695.

Table 4 shows the experimental values of f_{cc}/f_{co} and ε_{cc} compared with the theoretical ones according to this model, considering an effective strain coefficient k_ε=0.6. The error in estimating the compressive strength ranges between −3% and +29%, with a mean error of +12.2%. The ultimate theoretical strain is lower than the experimental strain in all cases with an average error of −35.3%.

The use of a form factor α_e=k_{s1}=k_{s2}=0.333 leads to larger errors underestimating the resistance with an average error of −19%.

Figure 7 shows the stress-strain curves recorded in the tests for specimens of series 2 and 3, and the theoretical curves according to the model. The model gives a good prediction for the strength, but the predicted slope of the second branch is greater than the experimental slope and thus the ultimate axial strain is underestimated.

5. CONCLUSIONS

This paper presents an experimental programme on the behaviour of low strength square concrete columns confined with FRP under axial compression.

TABLE 4. Comparison of the experimental results with the Lam and Ten'sg model (α_e=0.695 y k_ε=0.6)

	f_{cc}/f_{co}		ε_{cc}	
Specimen	**Exper.**	**Lam and Teng**	**Exper.**	**Lam and Teng**
C1	2.53	2.45	–	0.0241
G1	2.20	2.35	0.0287	0.0315
C2	1.81	1.98	0.0413	0.0175
G2	1.48	1.91	0.0351	0.0224
C3	1.71	1.77	0.0312	0.0145
G3	1.51	1.72	0.0197	0.0184
C4	1.74	1.76	0.0242	0.0144
G4	1.45	1.71	0.0237	0.0182
C5	1.48	1.73	0.0289	0.0139
G5	1.40	1.68	0.0286	0.0176
ERROR(%)		12.2		35.3

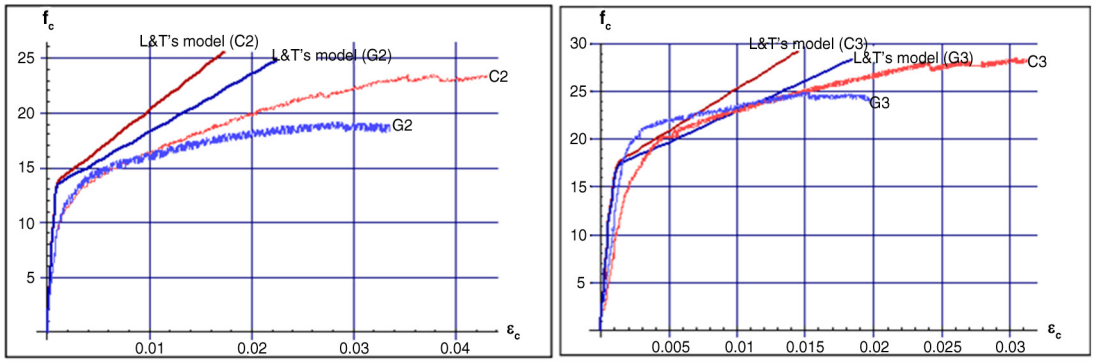

FIGURE 7. Comparison between experimental stress-strain curves and Lam and Teng's model.

The results were compared with the predictions of the more accepted theoretical models. There are too many factors which influence the behaviour of FRP confined concrete, so the following conclusions must be considered within the parameters used in the study.

Confinement with FRP composites can significantly improve the bearing capacity and ductility of square section reinforced concrete columns with rounded corners. The strength enhancement ratio is greater the lower the concrete strength and also increases with the stiffness of the jacket.

The stress-strain response of FRP confined concrete is approximately bilinear with a smooth transition zone. In the first region the behaviour is similar to that of unconfined concrete, while in the second zone it depends primarily on the stiffness of the FRP jacket. With rounded corners and sufficient confinement ratio (f_l/f_{co}) the second branch of the curve is also monotone upward, it being steeper the higher the stiffness of the jacket.

The failure occurs by tensile rupture of the jacket fibres to a strain value much lower than that obtained by tensile testing of FRP coupons.

Regarding the comparison carried out with the theoretical models, there are two key parameters for defining the behaviour of confined columns: the ratio between the tensile strength of the fibres in the jacket and in the testing of flat coupons; and the effect of confinement in non-circular sections. These parameters critically influence the fitting of the models.

There is not a theoretical approach or a clear experimental data base to easily establish these parameters. The two theoretical models analysed predict the general behaviour of the confined columns reasonably well. The Spoelstra and Monti's model including k_ε=0.6 and shape coefficient proposed by Mirmiran (α_e=2R$_c$/b=0.333) performs better in predicting the shape of stress-strain curves (mainly the slope of the second branch) of the specimens tested. The fit of this model could be improved with a better calibration of the above two parameters based on a larger experimental database.

ACKNOWLEDGMENTS

This study has been partially funded by the Spanish Ministry of Economy and Competitiveness (Project BIA2013-49103-C2-1-R).

REFERENCES

1. Bakis, C.; Bank, L.; Brown, V.; Cosenza, E.; Davalos, J.; Lesko, J.; Machida, A.; Rizkalla, S.; Triantafillou, T. (2002) Fiber-Reinforced Polymer Composites for Construction—State-of-the-Art Review. *J. Compos. Constr*. 6 [2], 73–87. http://dx.doi.org/10.1061/(ASCE)1090-0268(2002)6:2(73).
2. Perera, R.; Sevillano, E.; Arteaga, A.; de Diego, A. (2014) Identification of intermediate debonding damage in FRP-plated RC beams based on multi-objective particle swarm optimization without updated baseline model. *Compos. Part B: Eng*. 62, 205–217. http://dx.doi.org/10.1016/j.compositesb.2014.02.008.
3. Panjehpour, M.; Ali, A.A.A.; Voo, Y.L.; Aznieta, F.N. (2014) Modification of strut effectiveness factor for reinforced concrete deep beams strengthened with CFRP laminates. *Mater. Construcc*. 64 [314], e016. http://dx.doi.org/10.3989/mc.2014.02913.
4. Alzate, A.; Arteaga, A.; de Diego, A.; Cisneros, D.; Perera, R. (2013) Shear strengthening of reinforced concrete members with CFRP sheets. *Mater. Construcc*. 63 [310], 251–265. http://dx.doi.org/10.3989/mc.2012.06611.
5. *fib* Bulletin 14, Externally bonded FRP reinforcement for RC structures. The International Federation for Structural Concrete, Lausanne, Switzerland, (2001).
6. CNR-DT200/2004, Guide for the design and construction of externally bonded FRP systems for strengthening existing structures, Advisory Committee on Technical Recommendations for Construction, National Research Council, Rome, Italy, (2004).
7. ACI 440.2R-08, Guide for the design and construction of externally bonded FRP systems for strengthening concrete structures, American Concrete Institute Farmington Hills, Michigan, USA, (2008).
8. Concrete Society. Design guidance for strengthening concrete structures with fibre composite materials, 3rd ed., Concrete Society Technical Report No. 55, Crowthorne, Berkshire (UK), (2012).
9. Samaan, M.; Mirmiran, A.; Shahawy, M. (1998), Model of Concrete Confined by Fiber Composites. *J. Struct. Eng*. 124 [9], 1025–1031. http://dx.doi.org/10.1061/(ASCE)0733-9445(1998)124:9(1025).
10. Toutanji, H.A. (1999) Stress-Strain Characteristics of Concrete Columns externally Confined with Advanced Fiber Composite Sheets. *ACI Mat. J*. 96 [3], 397–404. http://dx.doi.org/10.14359/639.

11. Lam, L; Teng, J. G. (2003) Design-oriented Stress-Strain Model for FRP-confined Concrete. *Constr. Build. Mat*. 17, 471–486. http://dx.doi.org/10.1016/S0950-0618(03)00045-X.
12. Spoelstra, M. R.; Monti, G. (1999) FRP-Confined Concrete Model. *J. of Compos. Constr*. 3 [3], 143–150. http://dx.doi.org/10.1061/(ASCE)1090-0268(1999)3:3(143).
13. Mirmiran, A.; Shahawy, M. (1997) Behavior of Concrete Columns Confined by Fiber Composites. *J. Struct. Eng*. 123 [5], 583–590. http://dx.doi.org/10.1061/(ASCE)0733-9445(1997)123:5(583).
14. Teng, J.G.; Huang, Y.L.; Lam, L.; Ye, L.P. (2007) Theoretical model for fiber-reinforced polymer-confined concrete. *J. Compos. Constr*. 11 [2], 201–210. http://dx.doi.org/10.1061/(ASCE)1090-0268(2007)11:2(201).
15. Hu, H.; Seracino, R. (2014) Analytical Model for FRP-and-Steel-Confined Circular Concrete Columns in Compression. *J. Compos. Constr*. 18, Special Issue: 10th Anniversary of IIFC, A4013012. http://dx.doi.org/10.1061/(ASCE)CC.1943-5614.0000394.
16. Aire, G.; Gettu, R.; Casas, J.R.; Marques, S.; Marques, D. (2010) Concrete laterally confined with fibre-reinforced polymers (FRP): experimental study and theoretical model. *Mater. Construcc*. 60 [297], 19–31. http://dx.doi.org/10.3989/mc.2010.45608.
17. De Lorenzis, L.; Tepfers, R. (2003) Comparative Study of Models on Confinement of Concrete Cylinders with Fiber-Reinforced Polymer Composites. *J. Compos. Constr*. 7 [3], 219–237. http://dx.doi.org/10.1061/(ASCE)1090-0268(2003)7:3(219).
18. Chaallal, O.; Hassan, M.; Leblanc, M. (2006) Circular Columns Confined with FRP: Experimental versus Predictions of Models and Guidelines. *J. Compos. Constr*. 10 [1], 4–12. http://dx.doi.org/10.1061/(ASCE)1090-0268(2006)10:1(4).
19. Lim, J.C.; Ozbakkaloglu, T. (2014), Lateral Strain-to-Axial Strain Relationship of Confined Concrete, *J. Struct. Eng*., *10.1061/(ASCE)ST.1943-541X.0001094, 04014141*. http://dx.doi.org/10.1061/(ASCE)ST.1943-541X.0001094.
20. Chaallal, O.; Shahawy, M.; Hassan, M. (2003) Performance of Axially Loaded Short Rectangular Columns Strengthened with Carbon Fiber-Reinforced Polymer Wrapping. *J. Compos. Constr*. 7 [3], 200–208. http://dx.doi.org/10.1061/(ASCE)1090-0268(2003)7:3(200).
21. Rochette, P.; Labossière, P. (2000) Axial Testing of Rectangular Column Models Confined with Composites. *J. Compos. Constr*. 4 [3] 129–136. http://dx.doi.org/10.1061/(ASCE)1090-0268(2000)4:3(129).
22. Pham, T.M.; Doan, L.V.; Hadi, N.S. (2013) Strengthening square reinforced concrete columns by circularisation and FRP confinement. *Constr. Build. Mat*. 49, 490–499. http://dx.doi.org/10.1016/j.conbuildmat.2013.08.082.
23. Lam, L.; Teng, J.G. (2003) Design-Oriented Stress-Strain Model for FRP-Confined Concrete in Rectangular Columns. *J. Reinf. Plast. Compos*. 22 [13], 1149–1186. http://dx.doi.org/10.1177/0731684403035429.
24. EN ISO 527-4:1997 Plastics. Determination of tensile properties. Test conditions for isotropic and orthotropic fibre-reinforced plastic composites.
25. Pessiki, S.; Harries, K.A.; Kestner, J.; Sause, R.; Ricles, J.M. (2001) The axial behaviour of concrete confined with fiber reinforced composite jackets. *J. Compos. Constr*. 5 [4], 237–245. http://dx.doi.org/10.1061/(ASCE)1090-0268(2001)5:4(237).
26. Chen, J.F.; Li, S.Q.; Bisby, L.A.; Ai, J. (2011) FRP rupture strains in the split-disk test. Compos. B Eng. 42 [4], 962–972. http://dx.doi.org/10.1016/j.compositesb.2010.12.015.
27. Mander, J.B.; Priestley, M.J.N.; Park, R. (1988) Theoretical Stress-Strain Model for Confined Concrete. *J. Struct. Eng*. 114 [8], 1804–1826. http://dx.doi.org/10.1061/(ASCE)0733-9445(1988)114:8(1804).
28. Matthys, S.; Toutanji, H.; Audenaert, K.; Taerwe, L. (2005) Axial Load Behavior of Large-Scale Columns Confined with Fiber-Reinforced Polymer Composites. *ACI Struct. J*. 102 [2], 258–267. http://dx.doi.org/10.14359/14277.
29. Mirmiran, A.; Shahawy, M.; Samaan, M.; El Echary, H.; Mastrapa, J.C.; Pico, O. (1998) Effect of Column Parameters on FRP-Confined Concrete. *J. Compos. Constr*. 2 [4], 175–185. http://dx.doi.org/10.1061/(ASCE)1090-0268(1998) 2:4(175).
30. Karam, G.; Tabbara, M. (2004) Corner Effects in CFRP-Wrapped Square Columns. *Mag. Conc. Res*. 56 [8], 461–464. http://dx.doi.org/10.1680/macr.2004.56.8.461.